Red rock and red planet diagenesis: Comparisons of Earth and Mars concretions

Marjorie A. Chan, Brenda Beitler Bowen, W.T. Parry, *Department of Geology and Geophysics, University of Utah, 135 S 1460 E, Salt Lake City, Utah 84112-0111, USA, chan@earth.utah.edu, bbeitler@mines.utah.edu;* ***Jens Ormö,*** *Centro de Astrobiología, Instituto Nacional de Técnica Aeroespacial–Consejo Superior de Investigaciones Científicas (INTA-CSIC), Centra de Torrejón a Ajalvir, km 4, 28850 Torrejón de Ardoz, Madrid, Spain; and* ***Goro Komatsu,*** *International Research School of Planetary Sciences, Università d'Annunzio, Viale Pindaro 42, 65127 Pescara, Italy*

ABSTRACT

Compelling similarities between concretions on Earth and "blueberries" on Mars are used to suggest the blueberries are concretions that formed from a history of watery diagenesis. In the terrestrial examples, groundwater flow produces variations in sandstone color and iron oxide concretions in the Jurassic Navajo Sandstone of Utah. Variations in concretion mineralogy, form, and structure reflect different conditions at chemical reaction fronts, the influence of preferential fluid flow paths, the relative roles of advection and diffusion during precipitation, the presence of multiple events, fluid geochemistry, and time. The terrestrial concretions are analogs that can be used to understand the water-saturated conditions that formed spherical hematite concretions on Mars.

Keywords: diagenesis, concretions, hematite, goethite, Mars, Navajo Sandstone.

INTRODUCTION

The dramatic red Mesozoic sandstones in the southwestern desert of the United States often evoke images of the red planet, Mars. Understanding the evolution of red rock diagenesis on Earth could provide insights on the geologic history of Mars. Some of the most intriguing discoveries from the 2004 National Aeronautics and Space Administration (NASA) Mars Exploration Rover (MER) *Opportunity* images were the abundant accumulations of spherical balls (<0.5 cm diameter) of hematite. These spherical forms were dubbed "blueberries" because their distribution in the host rock was similar to blueberries in a muffin (Squyres et al., 2004).

Similar spherical balls are common on Earth as concretions, and many resemble marbles in size and shape. Concretions are concentrated mineral masses of a minor component precipitated in pores of sediments and sedimentary rocks (e.g., Mozley, 2003). Although there is no perfect Earth analog for the unique sedimentary system discovered at Meridiani Planum (e.g., basaltic host rock, evaporite cements, pure hematite concretions; Squyres et al., 2004), the Navajo Sandstone in southern Utah contains some of the world's most abundant and diverse examples of spheroidal iron oxide concretions and can be used to evaluate complex diagenetic concretion-forming processes.

This paper builds on previous work (Chan et al., 2004; Ormö et al., 2004) to highlight how interpretation of the new detailed Mars data requires a solid knowledge of Earth analogs and processes. Interdisciplinary studies of sedimentology and diagenesis from the terrestrial realm can yield valuable insights for understanding planetary geology. Despite differences in host rock, water types, sources of iron, burial history, and fluid flow timing, diagenesis on both Mars and Earth led to the formation of spherical hematite concretions. We present our model of red rock diagenesis from Utah examples, compare remarkable forms between Earth and Mars, and discuss the implications of the terrestrial analog for understanding Mars.

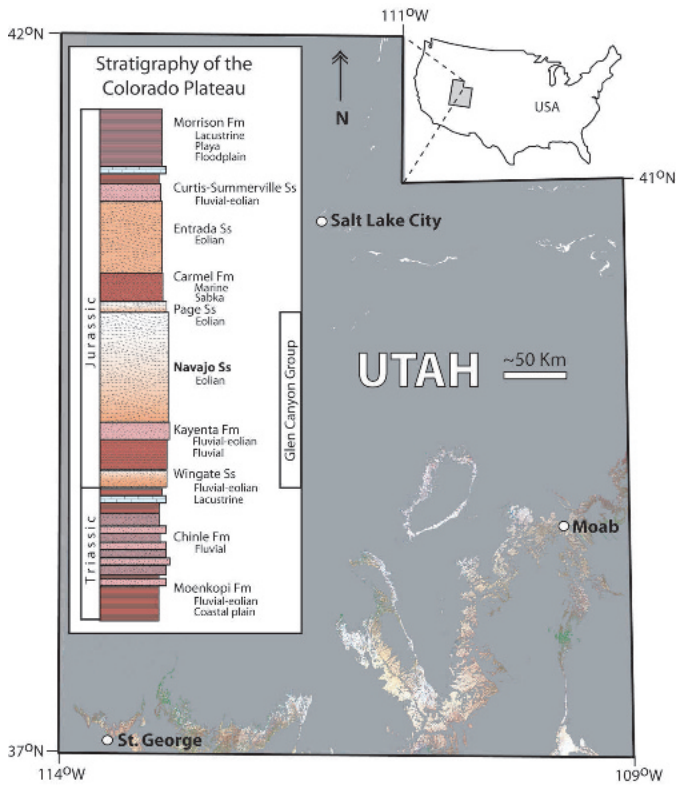

Figure 1. Locality map and stratigraphic section of southern Utah. Early Jurassic Glen Canyon Group (including the Navajo Sandstone) outcrops primarily exposed along Laramide uplifts. Outcrop color patterns from Landsat 7 ETM+ (bands 7, 4, 2) satellite imagery. Green indicates vegetation. Stratigraphic section shows typical outcrop colors.

GSA Today: v. 15, no. 8, doi: 10:1130/1052-5173(2005)015<4:RRARPD>2.0.CO;2

RED ROCK DIAGENESIS

The Lower Jurassic Navajo Sandstone is a well-exposed and widespread eolian unit in southern Utah (Fig. 1) with conspicuous color variations and a variety of iron oxide concretions. It is well known that sandstone color variations are due to different amounts of iron oxide (Cornell and Schwertmann, 2003), but the mechanisms of diagenesis and relationships to fluid flow and concretions have only recently been recognized (Chan et al., 2000; Chan and Parry, 2002; Beitler et al., 2003, 2005; Parry et al., 2004). Our studies of field relationships, petrography, geochemistry, mineralogy, and geochemical modeling provide the basis for analyzing fluid flow history within this system.

The Navajo Sandstone is one of the most porous and permeable units of the Colorado Plateau and therefore is a conduit for fluid movement, creating favorable conditions for the formation of concretions. The well-sorted, fine- to medium-grained eolian quartz arenite is composed of framework grains that are typically ~90% quartz, ~5% potassium feldspar, and ~5% clays and other accessory minerals (Beitler et al., 2005). Effective porosity averages ~17% (Cordova, 1978), and permeability can be up to 1 Darcy (Lindquist, 1988) with the coarser-grained grain flow laminae having higher permeabilities than the finer-grained and more clay-rich wind ripple laminae. Cement volumes typically comprise a few percent in unaltered Navajo Sandstone to as much as 35% in the concretions (Beitler et al., 2005). The conditions for formation of Utah concretions are interpreted to be diagenetic based on Navajo Sandstone burial estimates (Chan et al., 2004) and lack of high-temperature evidence or mineral assemblages.

Navajo Sandstone color variation and iron mineralization can be summarized as a three-step process of diagenetic stages involving groundwater flow, based on synthesis of material previously presented in several papers (e.g., Chan et al., 2000, 2004; Chan and Parry, 2002; Beitler et al., 2003; Parry et al., 2004).

1. *Iron source.* The source of iron is the initial breakdown of detrital Fe-bearing silicate minerals within the sandstone during interaction with meteoric waters. Thin iron oxide films coat individual sand grains shortly after deposition or during early burial (Berner, 1969). The thin hematite films typically comprise 0.18–1.25 wt% (Beitler et al., 2005) of the whole rock and impart a pink to orange-red color to the sandstone (Fig. 2A).
2. *Iron mobilization.* After burial and early cementation (e.g., calcite, quartz overgrowths), reducing fluids derived from underlying units move through the porous sandstone and remove the iron oxide films (Fig. 2B–C). The

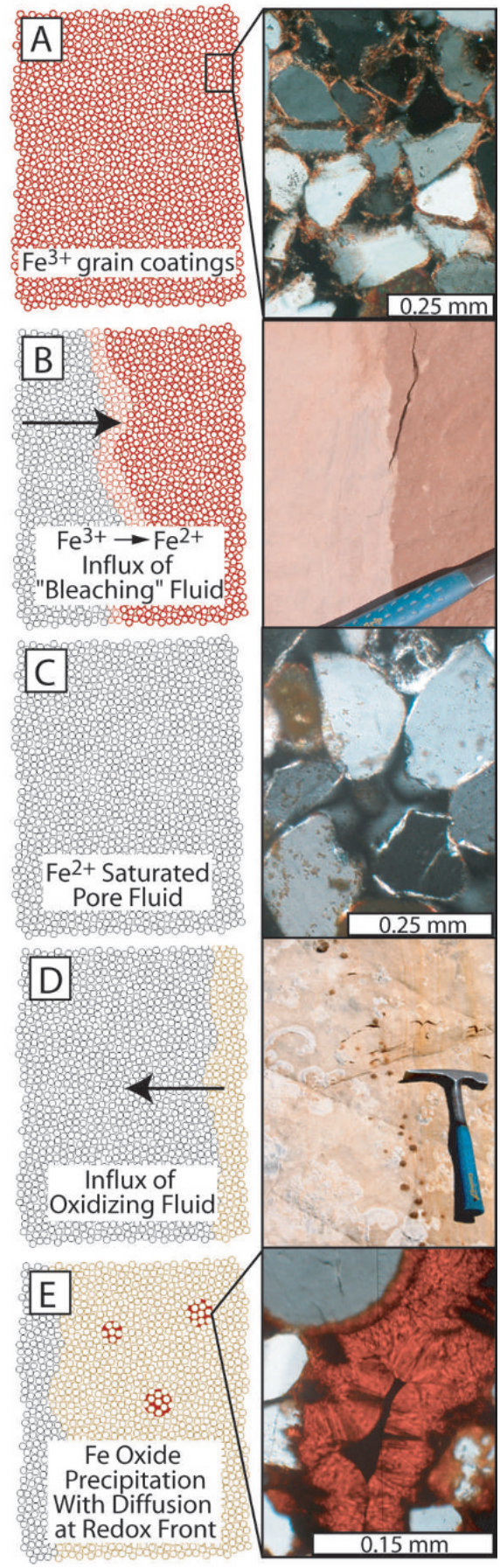

Figure 2. Grain scale model for terrestrial examples of Navajo Sandstone concretion formation. (A) Early hematite (Fe^{3+}) grain coatings; photomicrograph of hematite films around grains. (B) Influx of reducing fluids effectively "bleach" the buried sandstone. (C) Bleached sandstone pores are saturated with waters containing reduced iron (Fe^{2+}); photomicrograph of bleached sandstone lacking hematite grain coatings. (D) Influx of oxidizing groundwater creates redox front where concretions precipitate. (E) Concretions form along front with organized distribution and spherical shape; photomicrograph of cementing fibrous goethite crystals filling pore space to make the concretion.

reducing fluids effectively bleach the sandstone white, leaving <0.5 wt% iron oxide (Beitler et al., 2005). The reducing fluids may also reduce sulfate to sulfide and precipitate some of the iron as pyrite. Previous work on the Navajo Sandstone suggested that the reducing fluids are likely hydrocarbons (petroleum or methane) (Chan et al., 2000). Bleaching occurs on millimeter (Parry et al., 2004) to regional (Beitler et al., 2003) scales, reflecting the broad range of heterogeneities that can control fluid flow.

3. *Concretion precipitation.* Reducing fluids that carry the iron eventually mix with oxidizing groundwater (Fig. 2D–E). Under phreatic conditions where all the pores are saturated with the reducing fluid, diffusion at the interface between the oxidizing and reduced solution causes oxidation of iron and precipitation of concentrated hematite and/or goethite cements (von Gunten and Schneider, 1991). If pyrite is present, it would also oxidize to goethite at this stage. Many different shapes, such as bulbous nodules, pipes, sheets, and banding occur (Fig. 3), but the most common form along a reaction front is spheroidal. Dating of related mineralization (Chan et al., 2001) suggests that some precipitation occurred ca. 25 Ma, but mineralization commonly appears episodic, and some mineralization may be younger.

This diagenetic model of mixing fluids to precipitate concretions is similar to uranium roll-front models (e.g., Adler, 1974; discussion in Beitler et al., 2005) where uranium precipitates at chemical reaction mixing fronts. However, uranium precipitates under reducing conditions and is mobile under oxidizing conditions, the reverse of iron (Fig. 4). In the iron oxide model presented here, it is important to recognize this is an open chemical system with many complexities, including kinetic barriers, nucleation, mass transport, heterogeneities, and lack of equilibrium.

Concretion growth is affected by two important components of mass transfer: advection and diffusion. Advective flow is necessary to supply the required amounts of reactant iron and is indicated by oriented concretionary flow forms (Fig. 5). Iron is transported to the sites of concretion formation in water as reduced (ferrous) iron. The iron is precipitated by oxidation at a mixing front where the oxidant is transported to the site in a separate solution. There are

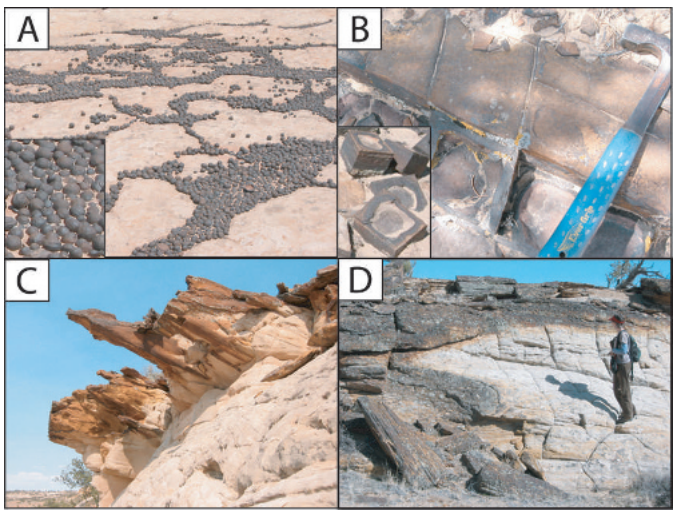

Figure 3. Diverse Utah concretionary forms due to different inherent host rock properties, anisotropies, and fluid flow characteristics. Concretion accumulations can act as geomorphic armor, protecting the underlying sandstone from erosion. (A) Spherical concretions (~3–5 cm diameter). (B) "Cinderblocks" from oxidizing fluids preferentially following horizontal stratification and vertical joint sets. (C) Subhorizontal pipes along bedding surface (pipes ~5 cm in diameter). (D) "Roll-front" type deposit.

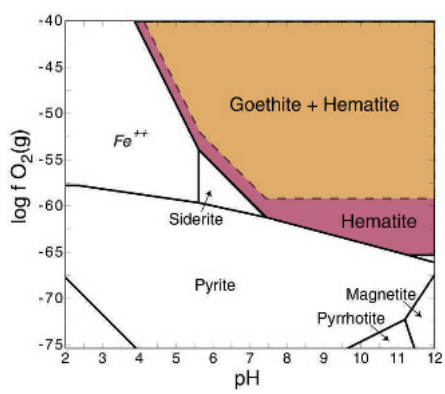

Figure 4. Phase diagram showing stability fields of iron oxides hematite and goethite at varying pH and fugacity of oxygen typical of Utah conditions where they form. Note that hematite and goethite occupy nearly identical areas due to similarity in free energy. Calculated at 50 °C, pressure = 1 atm, $a[Fe^{2+}] = 10^{-5}$, $a[H_20] = 1$, $a[SO_4^{-2}] = 10^{-2.57}$, $a[HCO_3^{-}] = 10^{-1.29}$, $a[Ca^{+2}] = 10^{-2.04}$, $a[Mg^{+2}] = 10^{-2.42}$, $a[Na^{+}] = 10^{-1.18}$. Activity scale in units of molality (mol/Kg). Compiled with the Geochemist's Workbench (Bethke, 1998).

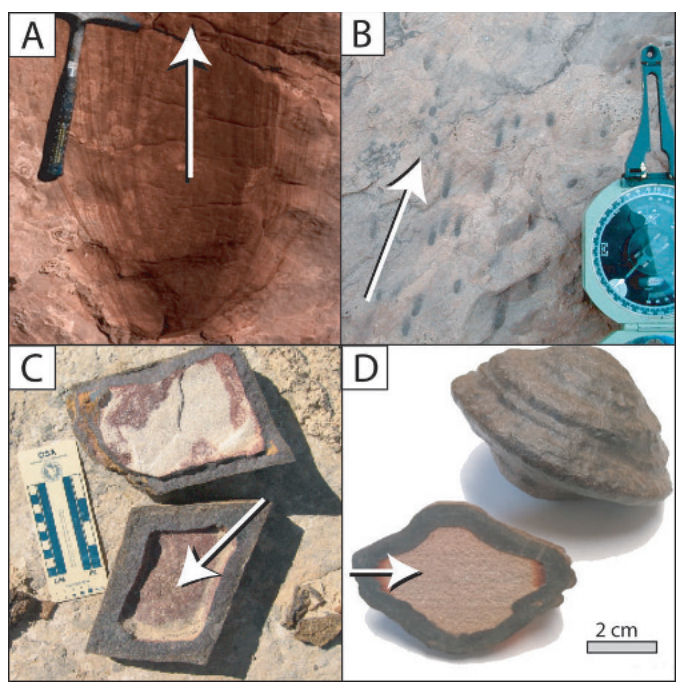

Figure 5. Flow patterns (arrows) indicated by preferential geometries in Navajo Sandstone concretions. (A–B) Advective flow indicated by strong asymmetric patterns. (C–D) Diffusive mass transfer indicated by inward directed patterns (left, along conjugate joints becoming less angular inward; right, "bleeding" along more permeable laminae).

insufficient amounts of iron and oxidant in a local volume of just the host rock alone to form an iron oxide concretion. Advection of reactants in two solutions is necessary.

Consider a spherical volume of porous rock 10 cm in diameter. If the water saturating the rock at 20% porosity contained 20 mg/kg Fe^{2+} (Parry et al., 2004) or 10 mg/kg O_2 (reasonable for air-saturated meteoric recharge water), the iron precipitate could amount to 3 mg of hematite or the O_2 could precipitate 10 mg of hematite. The amount of iron oxide in the Utah concretions exceeds this amount considerably. Therefore, both iron and oxygen must be supplied to the precipitation site advectively or by diffusion over large distances (several meters). Although advective mass transfer may be necessary for conditions that would support concretion growth, the spherical shapes and organized distribution suggests that diffusion of reactants from one solution to the other actually causes concretion precipitation (Berner, 1968, 1980).

UTAH-MARS SIMILARITIES

Hematite (Fe_2O_3) and iron oxide–hydroxide (e.g., goethite, FeOOH) nodules occur in a variety of geological settings and have a wide range of expressions, including pedogenic (Cescas et al., 1970; Schwertmann and Taylor, 1989; Stiles et al., 2001), oolitic (Van Houten and Bhattacharyya, 1982), and lakebed or seafloor nodules (Burns and Burns, 1975). Although a number of mechanisms can generate spherical shapes and iron oxide–rich nodules, the Utah concretions are consistent with more of the Mars blueberry characteristics and currently comprise a good analog for Mars blueberries for six reasons:

1. *Comparable hematite mineralogy.* X-ray diffraction and spectral analyses of Utah concretions show that different chemical reaction fronts from spatially distinct areas can have a range of compositional variations, including hematite and goethite (Chan et al., 2000; Beitler et al., 2005). The free energies of hematite and goethite are so close that either or both can precipitate (Majzlan et al., 2003) (Fig. 4). Iron solids typically precipitate at an oxic-anoxic boundary as polynuclear aggregates of Fe^{+3}

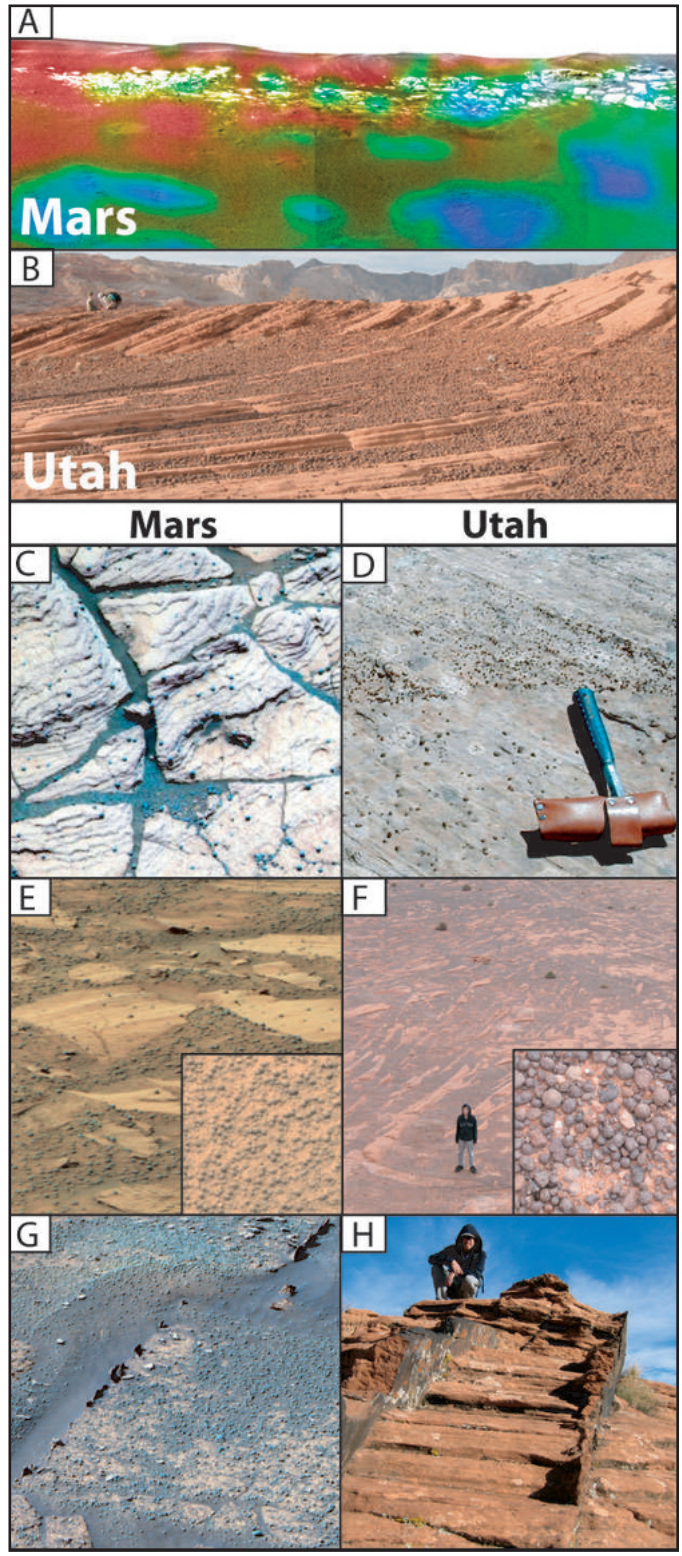

Figure 6. Comparisons of Mars and Utah examples. (A–B) Landscape scale. (C–D) In situ spherical concretions. (E–F) Weathered accumulations of spherical concretions. (G–H) Fracture-fill features. Mars examples (left) are compared with terrestrial images (right). (A) Mars Exploration Rover (MER) *Opportunity* panoramic view of Eagle Crater in Meridiani Planum region of Mars. Data from miniature thermal emission spectrometer superimposed on panoramic camera image. Superimposed colors indicate relative iron abundance: red and orange represent higher abundances than green and blue. Outcrop ledge (~1 m high) is relatively iron-poor, whereas accumulations of spherical objects ("blueberries") are iron-rich. Blue circular features in foreground show where the landing MER airbag bounced and buried the iron-rich spherical objects. Image credit: National Aeronautics and Space Administration (NASA)–Jet Propulsion Laboratory (JPL)–Arizona State University–Cornell. (B) Comparable Navajo Sandstone scene near St. George, Utah. Extensive bleached outcrop on the horizon, with weathered accumulation of iron oxide cemented spherical concretions (~2–4 cm diameter sizes) in the foreground. (C) False-color composite image of bedded "Shoemaker" outcrop in Eagle Crater, Mars. In situ spherical, iron-rich "blueberries" (~4 mm diameter) are embedded and regularly spaced within the sedimentary rock. Image credit: NASA–JPL–Cornell. (D) In situ Navajo Sandstone iron oxide concretions embedded within the sandstone at a similar spacing. Changes in permeability related to different types of eolian lamination commonly affect concretion spacing. (E) False color panoramic camera image in Endurance Crater, Mars. Inset shows weathered accumulation of spherical forms. Image credit: NASA–JPL–Cornell. (F) Navajo Sandstone plains covered by "blueberry"-sized iron oxide concretions, southwestern Utah. Inset shows weathered concretion accumulation (up to 1 cm diameter; most 3–6 mm diameter). (G) "Razorback" ridge that could be from diagenetic fracture fill in Endurance Crater, Mars. Feature is a few cm tall and <1 cm wide. Image credit: NASA–JPL–Cornell. (H) Iron oxide–cemented ridges from fluid flow along joint fractures in southwestern Utah.

hydroxides and ferrihydrite (Schwertmann and Fischer, 1973; von Gunten and Schneider, 1991). The original precipitate can convert to goethite, lepidocrocite, akaganeite, and finally to hematite (Berner, 1969). New studies suggest the Mars concretions were likely precipitated initially as goethite and dehydrated to hematite (Glotch et al., 2004; Tosca et al., 2005), similar to the Utah system. Mars hematite was suspected to be pure and crystalline based on spectral signatures (Christensen et al., 2001; Catling and Moore, 2003), which was confirmed by the distinctive six-peak hematite signature from in situ Mössbauer analysis at the *Opportunity* site (Klingelhöfer et al., 2004). Hematite concretions within the Navajo examples are typically fine-grained and red, in contrast to the pure, coarse-grained (gray) and crystalline concretions on Mars (Christensen et al., 2004; McLennan et al., 2005). The Utah concretions contain up to 35% iron oxide (Chan et al., 2000; Beitler et al., 2005), where nearly every mineral component is replaced by the hematite except for the very resistant quartz host grains. Similarly, the spherules in the "Berry Bowl" at the Eagle Crater, Meridiani, are reported to be replacive with up to 50% hematite and some remaining host rock component of basaltic mud and evaporite in the spherules (McLennan et al., 2005).

2. *Comparable size and self-organized in situ distribution.* The spherical forms in Utah and Meridiani have consistent and constrained size populations (Chan et al., 2004; McLennan et al., 2005). The distribution within the host rock is one of the key factors indicating that the Mars blueberries are concretions (Fig. 6). In nearly every other way that spherical terrestrial iron oxide nodules are generated (such as seafloor nodules, oolitic, or other), nodules would be clustered and touching, typically in a single bed. Instead, the concretion distribution suggests self-organization (Ortoleva, 1984, 1994) with a self-propagating, nearest-neighbor spacing. The Mars concretions appear to be contained within a specific geologic unit with consistent physical properties (Hynek et al., 2002). Although overall Navajo Sandstone spheroidal concretions range from mm-sized "blueberries" to >10 cm-sized "grapefruits," within any one reaction front population there is generally a consistent size. In general, small concretions are more closely spaced, and larger concretions are more widely spaced (Chan et al., 2004). The distribution of concretion sizes and their spacing is related to diffusion and density of nucleation sites. Thus, sparse large concretions form from a low number of nucleation sites, similar to textures in materials science and metamorphic porphyroblasts (e.g., Carlson et al., 1995).
3. *Comparable loose spherical forms in weathered accumulations.* Concretions are hard masses that are better cemented than the more easily weathered host rock and are collected in topographic lows because the round, loose marbles and blueberries can easily roll downhill (Fig. 6). The MER rock abrasion tool indicates the Mars blueberries are much more cemented than the surrounding host rock (Herkenhoff et al., 2004). Thus, the resistant balls collect on flat or topographically low places as a function of the weathering processes (e.g., eolian deflation lags) and inherent properties of the cementation (Soderblom et al., 2004). At the outcrop scale, iron oxides occur in relatively low amounts because the disseminated concretions are spread out within the host rock. Areas with higher iron oxide values occur where there are greater accumulations of concretions.

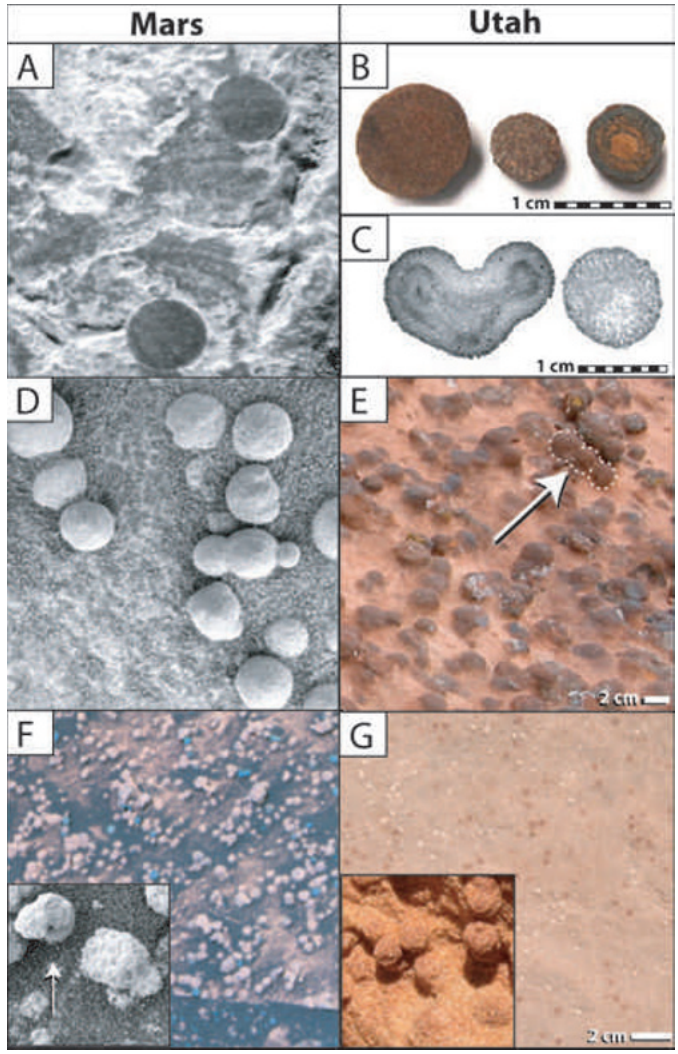

Figure 7. Comparison between internal structure and texture of Utah concretions and Mars "blueberries" (largest ones ~5 mm diameter). (A) Sliced Mars spherical forms showing relatively homogeneous internal structure. Image credit: National Aeronautics and Space Administration (NASA)–Jet Propulsion Laboratory (JPL)–Arizona State University–Cornell–U.S. Geological Survey (USGS). (B) Sliced (cross sectional) "blueberry"-sized Utah concretions showing relative homogeneous internal texture as well as concentric layered texture. (C) Microtomography displaying internal structure of Utah concretions. (D) Triplet of spherical forms from "Berry Bowl" in Eagle Crater, Mars. Image credit: NASA–JPL–Cornell–USGS. (E) Example of in situ concretion twins and triplets, Navajo Sandstone. (F) "Popcorn" texture coating associated with hematite-rich spherical forms in Endurance Crater, Mars. Image credit: NASA–JPL–Cornell. Inset: Detailed close-up showing hematite-rich spherical form embedded beneath the "popcorn" coating. Image credit: NASA–JPL–Cornell–USGS. (G) Weakly cemented Navajo concretions of both hematite (red) and carbonate (white) mineralogy. Inset: Weakly cemented terrestrial concretions with texture similar to Mars "popcorn."

4. *Comparable internal structure.* Although internal structures of other common concretions (e.g., carbonate) can show nuclei (Burns and Burns, 1975), the Utah Navajo Sandstone concretions and the Mars blueberries (Squyres et al., 2004) both lack an obvious macro nucleus (Fig. 7). An initial nucleus (such as a potassium feldspar or calcite grain in Utah sandstone) could be consumed in chemical reactions over time [e.g., H^+ consumption driving up pH to precipitate FeO(OH)] (Fig. 4). Many of the small, mm-sized terrestrial concretions typically show solid interiors, lacking obvious internal structure (Fig. 7B). The massive, solid interiors suggest fluid saturation and sufficient supply of the chemical reactants, balanced with the space for their growth (as opposed to outer rind types or "onion skin" types). With more time and perhaps multiple fluid-flow events, larger forms may grow. Within a given area and redox front, there can be thousands of small concretions. Some of the larger concretions typically exhibit layered internal structure, and some might have just one outer layer (from very thin, like an eggshell, to a thick rind) (Fig. 7B and 7C). Internal structure of the Utah concretions varies formation-wide, but is typically consistent within a specific reaction front population.
5. *Comparable geometric forms.* Both the Utah and Mars systems contain abundant spherical forms as well as some joined doublet and triplet forms (Fig. 7D and 7E). Where concretions nucleate in a homogeneous host rock by diffusive influx of solvents, the sphere is the most efficient (minimum free energy) form. In the Utah system, concretion size is at least partially a function of host rock properties. The spherical geometry and consistent size of the Mars concretions suggest the host rock is relatively homogeneous. The persistent occurrence of joined forms (e.g., doublets and triplets) can be attributed to nucleation phenomena, merging growth of adjacent spheres, or clustering as the diagenetic fluids move through the host rock. Navajo concretion triplets can form in a line or at angles (Fig. 7C and 7E). It is clear that variations in porosity and permeability have a strong influence on the formation of concretions (Seilacher, 2001). If anisotropies are present, mineralizing fluids tend to move preferentially along the paths with highest permeability (e.g., Mozley and Davis, 1996). Anisotropy of individual lamina can affect the fluid flow, and thus the spherical concretions may have a ridge-like feature around the periphery (Fig. 5D). Preferential cementation can occur as joint or fracture-fill as these provide conduits for migrating fluids. Cements precipitated along these pathways (whether iron oxide or other mineralogy) weather out as resistant "fins," akin to the dubbed "Razorback" recognized on Mars (Fig. 6G and 6H).
6. *Comparable variations in cementation.* Variations in cementation within the Mars system have created rough-texture forms dubbed "popcorn" by the MER team (McLennan et al., 2005). "Popcorn" concretions with a rough outer surface occur in the Utah analog where the concretion has a relatively low amount of cement and sometimes can show multiple diagenetic stages. In other words, "popcorn" may be a concretion form in which the iron oxide cement is only a few wt% versus more densely cemented concretions (Fig. 7F and 7G). "Popcorn" forms may have a hematite core, with more roughly textured portions of the concretions on the outside that can be interpreted as multiple cement generations (McLennan et al., 2005) and similarly can form in terrestrial examples.

COMPLEXITIES OF CONCRETION SYSTEM

There are clearly differences between Utah and Mars concretions. The Navajo concretions precipitate in a relatively chemically inert quartz arenite, where it is fairly straightforward to identify diagenetic mineralogy within the host rock pores. In the Meridiani environment, the host rock is more labile and potentially more involved in supplying the reactants for concretion formation (e.g., Catling, 2004; Clark et al., 2005; McLennan et al., 2005; Tosca et al., 2005). We infer that the Mars spherical forms are concretions that may have formed from mixing of an aqueous fluid that contained iron in solution and a separate oxidizing groundwater that precipitated hematite.

Occurrences of concretions in the Navajo Sandstone span many tens of kilometers, with variable conditions, expressions, and chemical reaction fronts, which all contribute to the diversity of forms. The Utah examples contain many shapes and sizes in comparison to Mars because (1) different tectonics, local porosity variations, and multiple fluid events have a notable effect; and (2) the *Opportunity* rover has traversed smaller areas and distances to date. The strength of the Utah examples in interpreting the Mars concretions is that the variability in the terrestrial system helps us to determine how different parameters affect the resulting concretions, and this in turn can help us isolate which parameters likely prevailed in concretion formation on Mars.

SUMMARY

Utah marble iron oxide concretions provide a valuable analog to help interpret spherical hematite blueberries on Mars. Although the singular aspect of the spherical geometry alone can be compared to a wide range of possible geologic Earth analogs where iron oxide occurs in nodular forms, the concretion model shows the most compelling comparisons to Mars. Both terrestrial marbles and Mars blueberries preserve a valuable stage of the diagenetic history that might not otherwise be present in the more extensive host rock. Variations on the terrestrial models help isolate potential controls on the processes, and these differences may be useful in distinguishing how and why the Mars blueberries are unique.

ACKNOWLEDGMENTS

We thank Gerry Ross, Laura Crossey, Scott McLennan, and Peter Mozley for their reviews and input on this manuscript. We thank Anthony Park of Sienna Geodynamics and Consulting Inc. for graphical contributions. We gratefully acknowledge donors to the American Chemical Society Petroleum Research Fund and the Bureau of Land Management Grand Staircase–Escalante National Monument for partial support of this research (to M.A.C. and W.T.P.). We acknowledge the successful efforts of the National Aeronautics and Space Administration Mars Exploration Rover

team; their images provide the basis for comparing the Martian results with the terrestrial analogs and will stimulate many future studies in understanding extraterrestrial processes.

REFERENCES CITED

Adler, H.H., 1974, Concepts of uranium-ore formation in reducing environments in sandstones and other sediments, *in* Formation of uranium ore deposits: Vienna, International Atomic Energy Agency, p. 141–168.

Beitler, B., Parry, W.T., and Chan, M.A., 2003, Bleaching of Jurassic Navajo Sandstone on Colorado Plateau Laramide highs: Evidence of exhumed hydrocarbon supergiants?: Geology, v. 31, p. 1041–1044, doi: 10.1130/G19794.1.

Beitler, B., Parry, W.T., and Chan, M.A., 2005, Fingerprints of fluid flow: Chemical diagenetic history of the Jurassic Navajo Sandstone, southern Utah: Journal of Sedimentary Research, v. 75, p. 545–559.

Berner, R.A., 1968, Rate of concretion growth: Geochimica et Cosmochimica Acta, v. 32, p. 477–483, doi: 10.1016/0016-7037(68)90040-9.

Berner, R.A., 1969, Goethite stability and the origin of red beds: Geochimica et Cosmochimica Acta, v. 33, p. 267–273, doi: 10.1016/0016-7037(69)90143-4.

Berner, R.A., 1980, Early diagenesis: A theoretical approach: Princeton, New Jersey, Princeton University Press, 241 p.

Bethke, C.M., 1998, The geochemist's workbench, version 3.0: Urbana, University of Illinois, 184 p.

Burns, R.G., and Burns, V.M., 1975, Mechanisms for nucleation and growth of manganese nodules: Nature, v. 255, p. 130–131.

Carlson, W.D., Denison, C., and Ketcham, R.A., 1995, Controls on the nucleation and growth of porphyroblasts—Kinetics from natural textures and numerical models: Geological Journal, v. 30, p. 207–225.

Catling, C., 2004, On Earth, as it is on Mars?: Nature, v. 429, p. 707–708, doi: 10.1038/429707a.

Catling, D.C., and Moore, J.M., 2003, The nature of coarse-grained crystalline hematite and its implications for the early environment of Mars: Icarus, v. 165, p. 277–300, doi: 10.1016/S0019-1035(03)00173-8.

Cescas, M.P., Tyner, E.H., and Harmer, R.S., III, 1970, Ferromanganiferous soil concretions: A scanning electron microscope study of their micropore structures: Soil Science Society of America Proceedings, v. 34, p. 641–644.

Chan, M.A., and Parry, W.T., 2002, Rainbow of rocks: Mysteries of sandstone colors and concretions in Colorado Plateau canyon country: Utah Geological Survey Public Information Series 77, 17 p.

Chan, M.A., Parry, W.T., and Bowman, J.R., 2000, Diagenetic hematite and manganese oxides and fault-related fluid flow in Jurassic sandstones, southeastern Utah: AAPG Bulletin, v. 84, p. 1281–1310.

Chan, M.A., Parry, W.T., Petersen, E.U., and Hall, C.M., 2001, ^{40}Ar-^{39}Ar age and chemistry of manganese mineralization in the Moab to Lisbon fault systems, southeastern Utah: Geology, v. 29, p. 331–334, doi: 10.1130/0091-7613(2001)029<0331:AAAACO>2.0.CO;2.

Chan, M.A., Beitler, B., Parry, W.T., Ormö, J., and Komatsu, G., 2004, A possible terrestrial analogue for hematite concretions on Mars: Nature, v. 429, p. 731–734, doi: 10.1038/nature02600.

Christensen, P.R., Morris, R.V., Lane, M.D., Bandfield, J.L., and Malin, M.C., 2001, Global mapping of Martian hematite mineral deposits: Remnants of water-driven processes on early Mars: Journal Geophysical Research, v. 106, E10, p. 23,873–23,885.

Christensen, P.R., Wyatt, M.B., Glotch, T.D., Rogers, A.D., Anwar, S., Arvidson, R.E., Bandfield, J.L., Blany, D.L., Budney, C., Calvin, W.M., Fallacaro, A., Fergason, R.L., Gorelick, N., Graff, T.G., Hamilton, V.E., Hayes, A.G., Johnson, J.R., Knudson, A.T., McSween, H.Y., Jr., Mehall, G.L., Mahall, L.K., Moersch, J.E., Morris, R.V., Smith, M.D., Squyres, S.W., Ruff, S.W., and Wolff, M.J., 2004, Mineralogy at Meridiani Planum from the Mini-TES experiment on the Opportunity Rover: Science, v. 306, p. 1733–1739, doi: 10.1126/science.1104909.

Clark, B.C., McLennan, S.M., Morris, R.V., Gellert, R., Jolliff, B., Knoll, A., Lowenstein, T.K., Ming, D.W., Tosca, N.J., Christensen, P.R., Yen, A., Bruckner, J., Calvin, W., Farrant, W., Zipfel, J., Gorevan, S., Squyres, S.W., and the Athena Science Team, 2005, Results and implications of mineralogical models for chemical sediments at Meridiani Planum: Houston, Lunar and Planetary Science Conference XXXVI, Abstract 1446, CD-ROM.

Cordova, R.M., 1978, Ground-water conditions in the Navajo Sandstone in the central Virgin River basin, Utah: Utah Department of Natural Resources Technical Publication 61, 66 p.

Cornell, R.M., and Schwertmann, U., 2003, The iron oxides: Structure, properties, reactions, occurrences and uses (revised and enlarged edition): Weinhem, Wiley-VCH, 664 p.

Glotch, T.D., Morris, R.V., Christensen, P.R., and Sharp, T.G., 2004, Effect of precursor mineralogy on the thermal infrared emission spectra of hematite: Application to Martian hematite mineralization: Journal of Geophysical Research, v. 109, E07003, doi: 10.1029/2003JE002224.

Herkenhoff, K.E., and 32 others, 2004, Evidence from Opportunity's microscopic imager for water on Meridiani Planum: Science, v. 306, p. 1727–1730, doi: 10.1126/science.1105286.

Hynek, B.M., Arvidson, R.E., and Phillips, R.J., 2002, Geological setting and origin of Terra Meridiani hematite deposit on Mars: Journal Geophysical Research, v. 107, E10, 5088, doi: 10.1029/2002JE001891.

Klingelhöfer, R.V., Morris, R.V., Bernhardt, B., Schröder, C., Rodionov, D.S., de Souza, P.A., Jr., Yen, A., Gellert, R., Evlanov, E.N., Zubkov, B., Foh, J., Bonnes, U., Kankeleit, E., Gütlich, P., Ming, D.W., Renz, F., Wdowiak, T., Squyres, S.W., and Arvidson, R.E., 2004, Jarosite and hematite at Meridiani Planum from Opportunity's Mössbauer spectrometer: Science, v. 306, p. 1740–1745, doi: 10.1126/science.1104653.

Lindquist, S.J., 1988, Practical characterization of eolian reservoirs for development: Nugget Sandstone, Utah Wyoming thrust belt: Sedimentary Geology, v. 56, p. 315–339, doi: 10.1016/0037-0738(88)90059-0.

Majzlan, J., Grevel, K.D., and Navrotsky, A., 2003, Thermodynamics of iron oxides: Part II: Enthalpies of formation and relative stability of goethite (a-FeOOH), lepidocrocite (g-FeOOH), and maghemite (g-Fe_2O_3): American Mineralogist, v. 88, p. 855–859.

McLennan, S.M., Bell, J.F., Calvin, W.M., Christensen, P.R., Clark, B.C., de Souza, P.A., Farrand, W.H., Fike, D., Gellert, R., Ghosh, A., Glotch, T.D., Grotzinger, J.P., Hahn, B., Herkenhoff, K.E., Hurowitz, J.A., Johnson, J.R., Johnson, S.S., Jolliff, B., Klingelhöfer, G., Watters, A.H., Wyatt, M.B., Yen, A., and the Athena Science Team, 2005, Provenance and diagenesis of impure evaporitic sedimentary rocks on Meridiani Planum, Mars: Houston, Lunar and Planetary Science Conference XXXVI, Abstract 1884, CD-ROM.

Mozley, P.S., 2003, Diagenetic structures, *in* Middleton, G., ed., Encyclopedia of sediments and sedimentary rocks: Dordrecht, Kluwer Academic Press, p. 219–225.

Mozley, P.S., and Davis, J.M., 1996, Relationship between oriented calcite concretions and permeability correlation structure in an alluvial aquifer, Sierra Ladrones Formation, New Mexico: Journal of Sedimentary Research, v. 66, p. 11–16.

Ormö, J., Komatsu, G., Chan, M.A., Beitler, B., and Parry, W.T., 2004, Geological features indicative of processes related to the hematite formation in Meridiani Planum and Aram Chaos, Mars: A comparison with diagenetic hematite deposits in southern Utah, USA: Icarus, v. 171, p. 295–316, doi: 10.1016/j.icarus.2004.06.001.

Ortoleva, P.J., 1984, The self organization of Liesegang bands and other precipitate patterns, *in* Nicolis, G., and Baras, F., eds., Chemical instabilities, applications in chemistry, engineering, geology, and materials science: NATO ASI series C: Mathematical and Physical Sciences: Dordrecht–Boston, D. Reidel Publishing, p. 289–297.

Ortoleva, P.J., 1994, Geochemical self-organization: New York, Oxford University Press, 432 p.

Parry, W.T., Chan, M.A., and Beitler, B., 2004, Chemical bleaching indicates fluid flow in sandstone deformation bands: AAPG Bulletin, v. 88, p. 175–191.

Schwertmann, U., and Fisher, W.R., 1973, Natural "amorphous" ferric hydroxide: Geoderma, v. 10, p. 234–247.

Schwertmann, U., and Taylor, R.M., 1989, Iron oxides, *in* Dixon, J.B., and Weed, S.B., eds., Minerals in soil environments: Madison, Wisconsin, Soil Science Society of America, p. 379–438.

Seilacher, A., 2001, Concretion morphologies reflecting diagenetic and epigenetic pathways: Sedimentary Geology, v. 143, p. 41–57, doi: 10.1016/S0037-0738(01)00092-6.

Stiles, C.A., Mora, C.I., and Driese, S.G., 2001, Pedogenic iron-manganese nodules invertisols: A new proxy for paleoprecipitation?: Geology, v. 29, p. 943–946, doi: 10.1130/0091-7613(2001)029<0943:PIMNIV>2.0.CO;2.

Soderblom, L.A., and 43 others, 2004, Soils of Eagle Crater and Meridiani Planum at the Opportunity rover landing site: Science, v. 306, p. 1723–1726.

Squyres, S.W., Grotzinger, J.P., Arvidson, R.E., Bell, J.F., III, Calvin, W., Christensen, P.R., Clark, B.C., Crisp, J.A., Farrand, W.H., Kerkenhoff, K.E., Johnson, J.R., Klingelhöfer, G., Knoll, A.H., McLennen, S.M., McSween, H.Y., Jr., Morris, R.V., Rice, J.W., Jr., Rieder, R., and Soderblom, L.A., 2004, In situ evidence for an ancient aqueous environment at Meridiani Planum, Mars: Science, v. 306, p. 1709–1714, doi: 10.1126/science.1104559.

Tosca, N.J., McLennan, S.M., Clark, B.C., Grotzinger, J.P., Hurowitz, J.A., Jolliff, B.L., Knoll, A.H., Schroder, C., Squyres, S.W., and the Athena Science Team, 2005, Geochemical modeling of evaporites on Mars: Insight from Meridiani Planum: Houston, Lunar and Planetary Science Conference XXXVI, Abstract 1724, CD-ROM.

Van Houten, F.B., and Bhattacharyya, D.P., 1982, Phanerozoic oolitic ironstones—Geologic record and facies model: Annual Review of Earth and Planetary Sciences, v. 10, p. 441–457, doi: 10.1146/annurev.ea.10.050182.002301.

von Gunten, U., and Schneider, W., 1991, Primary products of oxygenation of iron (II) at an oxic/anoxic boundary; nucleation, agglomeration, and aging: Journal of Colloid and Interface Science, v. 145, p. 127–139, doi: 10.1016/0021-9797(91)90106-I.

Manuscript received 2 March 2005; accepted 31 May 2005.